

CFD Simulation of Methane Jet Burner

L. Perković^{*1}, M. Baburić¹, P. Priesching², N. Duić¹

¹ Faculty of Mechanical Engineering and Naval Architecture,
University of Zagreb, Croatia

² AVL-AST, Graz, Austria

Abstract

Methane jet flame simulations have been performed in order to evaluate conserved scalar chemistry (CSC) approach in modelling combustion process inside cylindrical burner. Two combustion regimes were included: non-premixed and premixed. For both of them it was necessary to generate look-up tables in pre-processing stage. For non-premixed regime two combustion controlling parameter approaches were used: scalar dissipation rate and normalized reaction progress variable (nRPV) approach. For premixed regime only nRPV approach was used. As an addition to CSC module, discrete transfer radiation module (DTRM) radiation model was also included. Simulation results were compared with experimental data.

Introduction

Conserved scalar chemistry model is based on pre-tabulated chemistry (look-up tables). For fluid flow solver, AVL FIRE (v2008) was used. Look-up tables were generated in separate applications. Constraining values for interpolation from look-up tables were variables resolved from computational domain. Those are tracking scalars: mixture fraction mean (Z), mixture fraction variance (Z_{var}) and RPV (in case when tables were reparametrised with RPV).

The non-premixed tables for diffusion flames were generated with stationary laminar flamelet model (SLFM) [6] in CSC solver [8]. These tables were then re-parametrised with properly selected (normalised) reaction progress variable (nRPV) in order to generate SLFM-RPV tables. This is known as presumed conditional moment (PCM) closure approach.

Tables of freely propagating adiabatic premixed flames were generated with an adopted 1-D PREMIX solver [9]. These tables have also been re-parametrised with nRPV in PCM procedure and as a result one gets FPI-RPV tables. This is known as flame prolongation of intrinsic low-dimensional manifold (FPI) [12] approach.

In SLFM combustion controlling parameter is scalar dissipation rate which is resolved from flow field turbulence parameters k and ϵ . In both SLFM-RPV and FPI-RPV controlling parameter is RPV, which in this case was sum of CO_2 , CO and H_2O , as suggested from [5]. CHEMKIN II libraries [10] were used for chemical kinetics and species properties evaluations. K - ϵ turbulence model was used and turbulence/chemistry interaction was accomplished via the presumed β -PDF. Interpolation from β -PDF tables was done via tracking (active) scalars resolved from computational domain: Z and Z_{var} . In case where RPV approach is used, nRPV is used as a parameter, otherwise scalar dissipation rate was used. In order to capture radiative heat transport discrete transfer radiation module (DTRM) [14,15] was used with weighted sum of grey gases model [16].

Numerical solution was compared with experimental results from published by Sandia National Laboratories.

Comparison criteria was temperature and main species mass fractions in centerline axial and two radial directions. Fuel to air ratio is in this work described by mixture fraction Z , defined as:

$$Z = \frac{m_F}{m_F + m_O} \quad ()$$

where m_F is mass flow rate on fuel, and m_O on oxidizer side.

Experimental configuration

Experimental configuration consisted from a central fuel jet, a pilot jet and a co-flow air jet in a concentric annular arrangement (Figure 1).

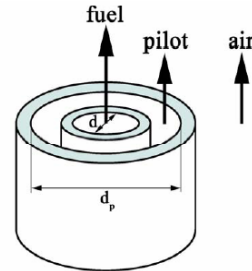


Figure 1. Methane flame configuration

The fuel was composed of 25% methane (CH_4) and 75% air by volume and had temperature 294 K. The surrounding pilot had an equivalent equilibrium composition to methane/air at $Z=0.27$, with the temperature 1880 K. The co-flowing air was held at 291 K. The flame operated at $\text{Re}=22400$ with a small degree of local extinction (Sandia flame D). The bulk velocities were 49.6 m/s for the fuel, 11.4 m/s for the pilot and 0.9 m/s for the air. Velocity profiles are presented in Figure 2.

* Corresponding author: luka.perkovic@fsb.hr

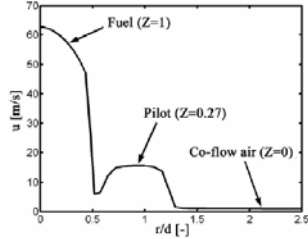


Figure 2. Inlet velocity profiles

Numerical set-up

A computational mesh consisted of 338400 control volumes covering a cylindrical domain from $x/d=0$ to $x/d=150$ in axial direction and from $r/d=0$ to $r/d=40$ in radial direction. The mesh was denser towards the central axis and inlets (Figure 3). The mesh density was similar to those from the simulations reported in TNF proceedings [1]. No mesh sensitivity analysis was performed.

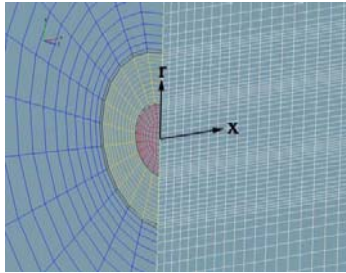


Figure 3. Computational mesh

The GRIMech 3.0 [2] chemical mechanism (53 species and 325 reactions) was used for chemical pre-tabulations.

The DTRM used 48 (4×12) rays per boundary cell. WSGGM was used for the radiative properties evaluations. As the flame was unconfined, the domain boundaries were considered as black surfaces ($\epsilon_b = 1$).

The constant $C_{\epsilon 2}$ in the transport equation for the dissipation rate of the turbulent kinetic energy was set to $C_{\epsilon 2} = 1.8$, as suggested in the TNF proceedings [1]. The inlet velocities were imposed according to experimental measurements (Figure 2). Turbulent kinetic energy at inlet boundaries was estimated from the experimental measurements of the Reynolds stresses. The dissipation rate of the turbulent kinetic energy was prescribed [3] as:

$$\epsilon = \sqrt{C_{\mu}} k \left| \frac{\partial u}{\partial r} \right| \quad (*)$$

Constant ambient pressure conditions were imposed at all outlet boundary selections. Incompressible solver was used and calculation was stationary. Convergence criteria was that normalized residuals for all equations must fall under 10^{-6} . The convection term in the continuity equation was discretized using the central differencing scheme (2nd order), while the same terms in the momentum equations were discretized using a hybrid between the central differences and the upwind

scheme (blending factor 0.5). The convection terms in the scalar equations were discretized using the upwind scheme (1st order). As usually, diffusion terms in all equations were discretized using the central differences. Other numerical set-up was as default in the FIRE solver [4]. Since nRPV approach includes one additional transport equation for RPV, boundary conditions of RPV were introduced through reaction rate of RPV in cells adjacent to boundary faces. Reaction rates were interpolated from look-up tables with respect to given value of boundary condition of Z , Z_{var} and temperature.

Pre-tabulated chemistry profiles

Following figures represent mixture fractions of two representative reactive scalars: methane and water (vapor).

The SLFM database (Figures 4, 5) was created for a range of the stoichiometric scalar dissipation rate parameters (14 profiles): $\chi_{st} = (0.01, 0.1, 1, 2, 5, 10, 20, 50, 100, 150, 200, 300, 450, 575)$. The first flamelet ($\chi_{st} = 0.01$) has a near-equilibrium composition, while the last one ($\chi_{st} = 575$) is nearly the last burning flamelet before extinction. The boundary species compositions and temperatures were imposed according to experimental data. The mixture fraction space was discretized into 50 non-equally distributed points, with a denser point distribution near the stoichiometry ($Z_{st} \approx 0.353$).

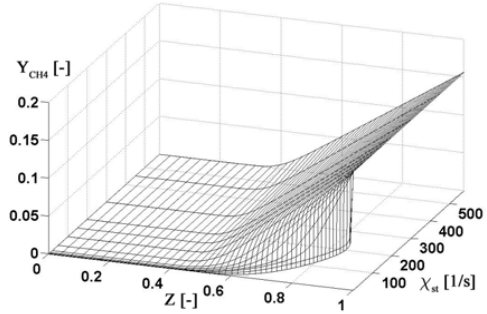


Figure 4. SLFM table for CH4

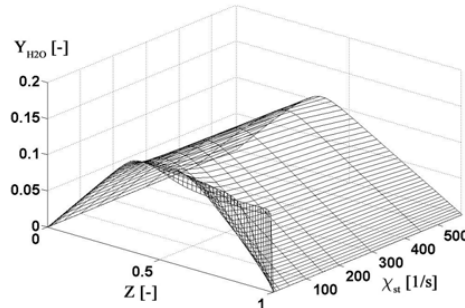


Figure 5. SLFM table for H2O

A linear combination of CO_2 , CO and H_2O mass fractions was used as the reaction progress variable, i.e. $Y_c \equiv Y_{CO_2} + Y_{CO} + Y_{H_2O}$ as suggested by [5]. The

flammable range was approximately $0.1673 \leq Z \leq 0.7968$ (Figure 6).

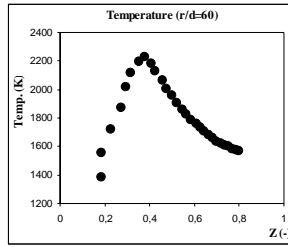


Figure 6. Burnt gas temperature vs. equivalence ratio

There were 29 premixed flames sets obtained within the flammability limits, while the remaining 21 sets were obtained by linear interpolation with boundary values. The mixture fraction discretization from the original SLFM database was retained. The FPI database is shown in Figures 7, 8.

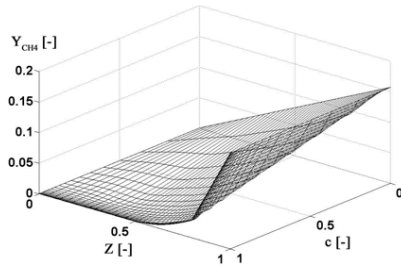


Figure 7. FPI-RPV table for CH4

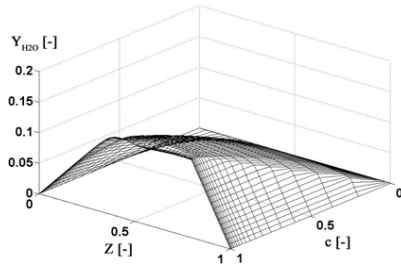


Figure 8. FPI-RPV table for H2O

Re-parameterised SLFM databases are shown in Figures 9 and 10.

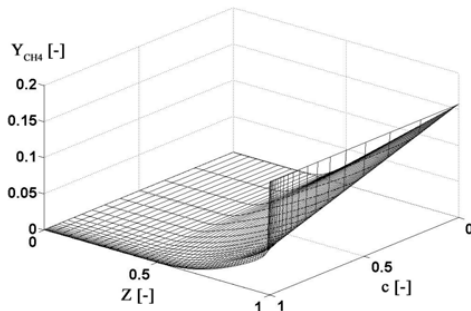


Figure 9 SLFM-RPV table for CH4

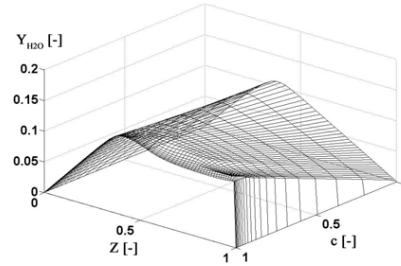


Figure 10. SLFM-RPV table for H2O

Results and Discussion

Resulting profiles are displayed along (centerline) axial direction and two radial directions on two axial positions: $x/d=30$ and $x/d=60$. Temperature is presented first, followed by mass fractions of representative species: CH4, O2, H2O and NO.

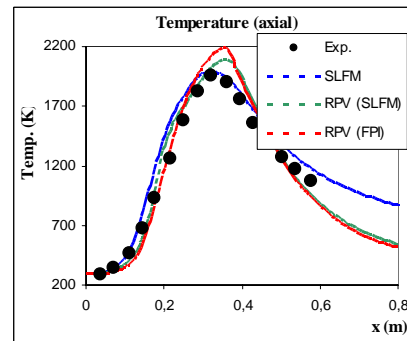


Figure 11. Axial temperature profile

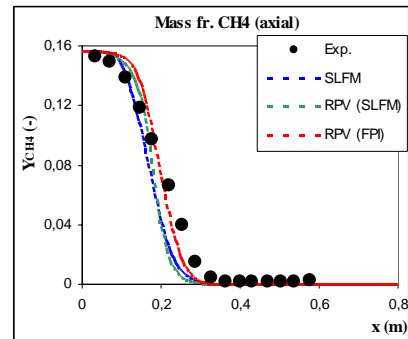


Figure 12. Axial profile of CH4

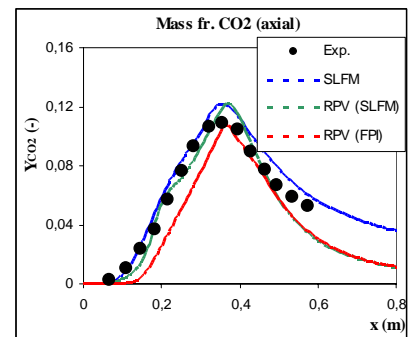


Figure 13. Axial profile of CO2

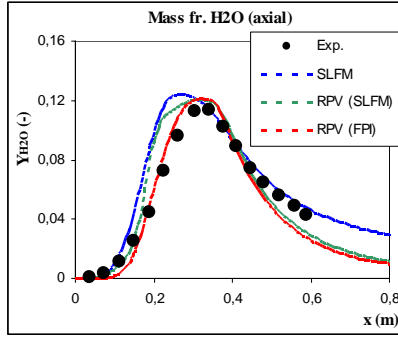


Figure 14. Axial profile of H2O

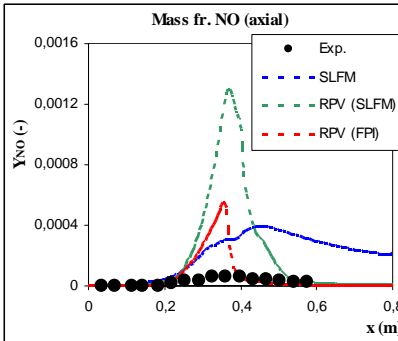


Figure 15. Axial profile of NO

Both RPV approaches overpredict temperature in range between 0.28 to 0.45 m (combustion zone), while SLFM remains close to experimental data (Figure 11). Above 0.4 m (fuel-lean zone) SLFM overpredicts temperature, while RPV approaches underpredict it. Profiles of CH₄ agrees well with experimental data along whole domain, except for slight underprediction in combustion zone (Figure 12). For both CO₂ and H₂O and for both RPV approaches concentrations are underpredicted in fuel-lean regions and slightly overpredicted in SLFM approach (Figure 13). NO is generally badly predicted by all models, but qualitatively RPV can show making and disappearing of NO in combustion zone. SLFM overpredicts NO in combustion and fuel-lean zone (Figure 14).

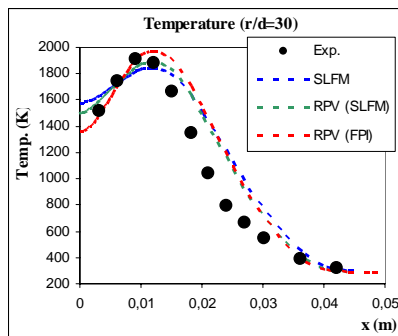


Figure 16. Radial temperature profile at $x/d=30$

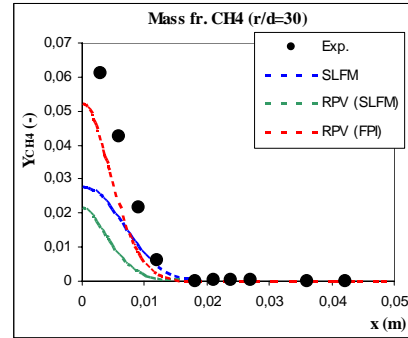


Figure 17. Radial profile of CH₄ at $x/d=30$

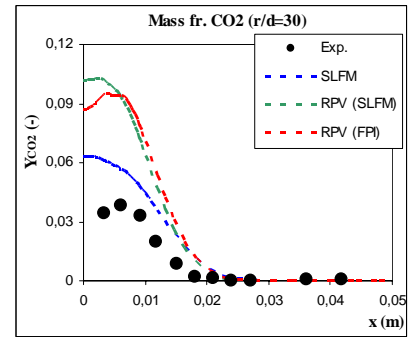


Figure 18. Radial profile of CO₂ at $x/d=30$

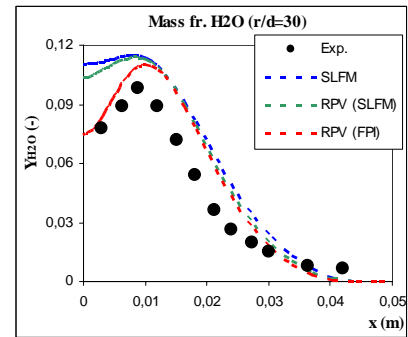


Figure 19. Radial profile of H₂O at $x/d=30$

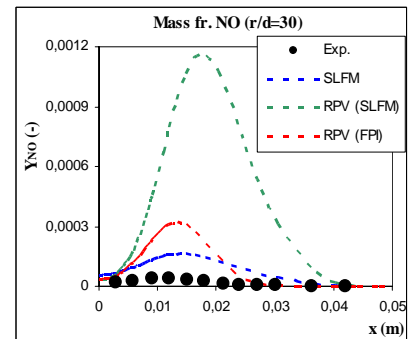


Figure 20. Radial profile of NO at $x/d=30$

Temperature is generally overpredicted (Figure 16) and CH₄ is generally underpredicted (Figure 17) by all three approaches. CO₂ and H₂O are slightly overpredicted

along whole profile (Figures 18 and 19). NO is again only qualitatively predicted (Figure 20).

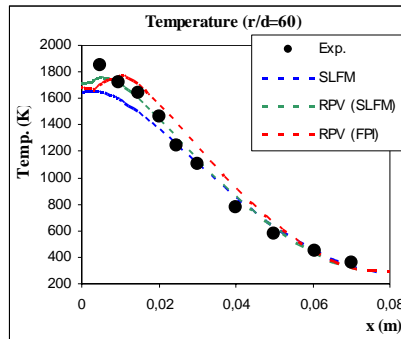


Figure 21. Radial temperature profile at $x/d=30$

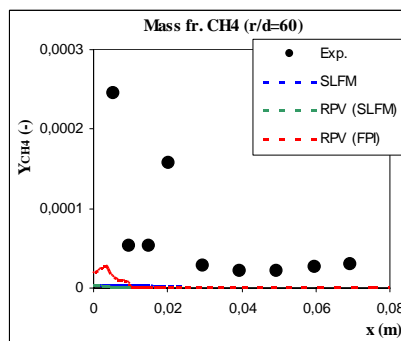


Figure 22. Radial profile of CH4 at $x/d=60$

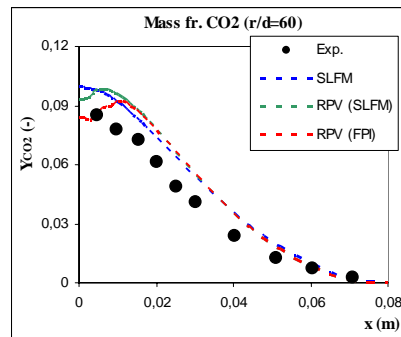


Figure 23. Radial profile of CO2 at $x/d=60$

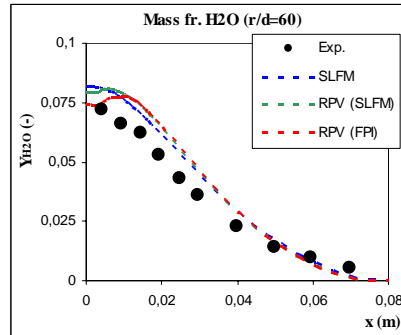


Figure 24. Radial profile of H2O at $x/d=60$

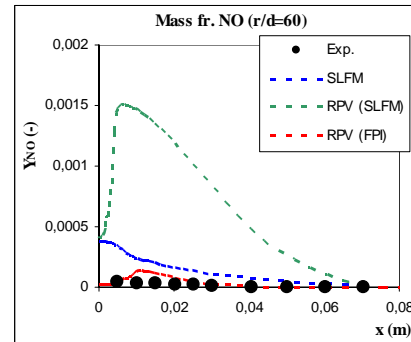


Figure 25. Radial profile of NO at $x/d=60$

All three models predict temperature well (Figure 21). CH4 (Figure 22) is very underpredicted along whole profile but CO2 and H2O are only slightly overpredicted (Figures 23 and 24). All three models predict NO very bad (Figure 25).

Conclusions

All three different combustion models (SLFM, SLFM-RPV and FPI-RPV) perform similar when considering major species, like CO2 and H2O, but show very bad prediction of NO. Temperature profiles can be predicted very good with all three approaches, but in order to get more accurate solution in species concentration one should take into account that all tables in pre-processing stage were done by assumption of adiabatic combustion, thus heat removal is not taken into account when generating species concentration tables.

References

- [1] <http://www.ca.sandia.gov/TNF/abstract.html>
- [2] http://me.berkeley.edu/gri_mech/
- [3] Hinz, A., "Numerische Simulation turbulenter Methandiffusionsflammen mittels Monte Carlo PDF Methoden", PhD thesis, Technische Universitaet Darmstadt, Darmstadt, 2000.
- [4] AVL AST, FIRE Manual v2008, AVL List GmbH, 2008.
- [5] Baburić, M., "Numerically efficient modelling of turbulent non-premixed flames", PhD thesis, University of Zagreb, Zagreb, 2005.
- [6] Peters, N., "Turbulent Combustion", Cambridge University Press, Cambridge, 2000.
- [7] Vervisch, L.; Hauguel, R.; Domingo, P. and Rullaud M., "Three facets of turbulent combustion modelling: DNS of premixed V-flame, LES of lifted nonpremixed flame and RANS of jet-flame", J. of Turbulence, 5 (2004), pp. 1-36
- [8] <http://powerlab.fsb.hr/mbaburic/CSC.htm>
- [9] Kee, R. J.; Grcar, J. F.; Smooke M. and Miller J. A., "A Fortran program for modelling steady laminar one-dimensional flames", SAND85-8240, Sandia National Laboratories, 1985.
- [10] Kee, R. J.; Rupley, F. M. and Miller J. A., "Chemkin II: A Fortran Chemical Kinetics Package"

for the Analysis of Gas-Phase Chemical Kinetics”, SAND89-8009, Sandia National Laboratories, 1989.

- [11] Barlow, R. S. and Frank, J. H., "Effects of turbulence on species mass fractions in methane/air jet flames", Proc. 27 th Symposium (International) on Combustion, The Combustion Institute, 1998.
- [12] Gicquel, O.; Darabiha, N. and Thévenin D., "Laminar premixed hydrogen/air counterflow flame simulations using flame prolongation of ILDM with differential diffusion", Proc. 28 th Symposium (International) on Combustion, The Combustion Institute, 2000.
- [13] Pierce, C. D., "Progress-variable approach for large-eddy simulation of turbulent combustion", PhD thesis, Department of Mechanical Engineering, Stanford University, 2001.
- [14] Lockwood, F. C. and Shah, N. G., "A new radiation solution for incorporation in general combustion prediction procedures", Proc. 18 th Symposium (International) on Combustion, The Combustion Institute, 1981.
- [15] Coelho, P. J. and Carvalho, M. G., "A Conservative Formulation of Discrete Transfer Method", ASME Journal of Heat Transfer, 119 (1997), pp. 118-128
- [16] Smith, P. J.; Shen, Z. F. and Friedman J. N., "Evaluation of Coefficients for the Weighted Sum of Gray Gas model", J Heat Transfer, 104, 1982.